







# Oligomerization of protein arginine methyltransferase 1 and its effect on methyltransferase activity and substrate specificity

Vincent Rossi<sup>1</sup>  | Sarah E. Nielson<sup>1</sup>  | Ariana Ortolano<sup>1</sup> |  
Isabella Lonardo<sup>1</sup>  | Emeline Haroldsen<sup>1</sup>  | Drake Comer<sup>1</sup> |  
Owen M Price<sup>1</sup>  | Nathan Wallace<sup>2</sup> | Joan M. Hevel<sup>1</sup> 

<sup>1</sup>Department of Chemistry and Biochemistry, Utah State University, Logan, Utah, USA

<sup>2</sup>NanoTemper Technologies, South San Francisco, California, USA

## Correspondence

Joan M. Hevel, Department of Chemistry and Biochemistry, Utah State University, 0300 Old Main Hill, Logan, UT 84322, USA.

Email: [joanie.hevel@usu.edu](mailto:joanie.hevel@usu.edu)

## Funding information

National Science Foundation,  
Grant/Award Numbers: CHE-2003769,  
MRI-1530862

**Review Editor:** Aitziber L. Cortajarena

## Abstract

Proper protein arginine methylation by protein arginine methyltransferase 1 (PRMT1) is critical for maintaining cellular health, while dysregulation is often associated with disease. How the activity of PRMT1 is regulated is therefore paramount, but is not clearly understood. Several studies have observed higher order oligomeric species of PRMT1, but it is unclear if these exist at physiological concentrations and there is confusion in the literature about how oligomerization affects activity. We therefore sought to determine which oligomeric species of PRMT1 are physiologically relevant, and quantitatively correlate activity with specific oligomer forms. Through quantitative western blotting, we determined that concentrations of PRMT1 available in a variety of human cell lines are in the sub-micromolar to low micromolar range. Isothermal spectral shift binding data were modeled to a monomer/dimer/tetramer equilibrium with an EC<sub>50</sub> for tetramer dissociation of ~20 nM. A combination of sedimentation velocity and Native polyacrylamide gel electrophoresis experiments directly confirmed that the major oligomeric species of PRMT1 at physiological concentrations would be dimers and tetramers. Surprisingly, the methyltransferase activity of a dimeric PRMT1 variant is similar to wild type, tetrameric PRMT1 with some purified substrates, but dimer and tetramer forms of PRMT1 show differences in catalytic efficiencies and substrate specificity for other substrates. Our results define an oligomerization paradigm for PRMT1, show that the biophysical characteristics of PRMT1 are poised to support a monomer/dimer/tetramer equilibrium in vivo, and suggest that the oligomeric state of PRMT1 could be used to regulate substrate specificity.

This is an open access article under the terms of the [Creative Commons Attribution-NonCommercial-NoDerivs](https://creativecommons.org/licenses/by-nc-nd/4.0/) License, which permits use and distribution in any medium, provided the original work is properly cited, the use is non-commercial and no modifications or adaptations are made.

© 2024 The Author(s). *Protein Science* published by Wiley Periodicals LLC on behalf of The Protein Society.

## KEYWORDS

arginine methylation, effect of oligomerization on activity, enzyme oligomerization, physiological concentrations, PRMT1, protein arginine methyltransferase, protein methylation, regulation of PRMT1 activity, substrate specificity

## 1 | INTRODUCTION

Protein arginine methylation is a predominant posttranslational modification in eukaryotic cells, with methylation occurring on 0.5%–4% of arginine residues in the mammalian proteome (Boffa et al., 1977; Bulau et al., 2006; Esse et al., 2014; Maron et al., 2021; Paik & Kim, 2006; Zhang et al., 2021). Arginine methylation is catalyzed by a family of protein arginine *N*-methyltransferases (PRMTs), which add one or two methyl groups to the guanidino nitrogen of arginine residues in targeted proteins using *S*-adenosyl-*L*-methionine (AdoMet) as a methyl donor. The PRMT family consists of nine members that are classified into three types (type I, II, or III), which are defined by whether the enzymes form monomethylated, asymmetric dimethylated, or symmetric dimethylated arginyl products (Morales et al., 2016; Tewary et al., 2019; Thiebaut et al., 2021). Protein arginine methylation of histone and non-histone proteins is important in a wide range of cellular processes including the regulation of DNA transcription, DNA damage repair, RNA processing and translation, and protein stability; aberrant arginine methylation is implicated in cardiovascular, neuromuscular, neurodegenerative, lung and cancer disease states (Al-Hamashi et al., 2020; Jarrold & Davies, 2019; Lorton & Shechter, 2019; Shen et al., 2024; Thiebaut et al., 2021; Xu & Richard, 2021), prompting a concerted effort to develop PRMT inhibitors (Dong et al., 2022; Hwang et al., 2021; Jarrold & Davies, 2019; Li et al., 2019; Shen et al., 2024).

PRMT1, a type I enzyme, is the predominant isoform in mammalian cells accounting for ~85% of total protein arginine methylation (Tang et al., 2000). Knockout of PRMT1 in mice results in embryo lethality (Pawlak et al., 2000) while altered PRMT1 protein expression has been reported in various types of cancer, including lung, breast, bladder, and pancreatic cancers (Feng et al., 2023; Filipović et al., 2019; He et al., 2020; Song et al., 2020; Wang et al., 2019; Yoshimatsu et al., 2011), as well as in idiopathic pulmonary fibroses (Lambers et al., 2019; Zakrzewicz et al., 2014; Zakrzewicz et al., 2015) and asthma (Park et al., 2021; Sun et al., 2017). The catalytic core of PRMT1 contains a Rossman fold that binds the cofactor AdoMet, a beta-barrel that is thought to be involved in substrate binding (Schapira & Ferreira de Freitas, 2014), and a dimerization arm. Crystallographic

structures reveal PRMT1 adopts a homo-dimeric state with a characteristic head-to-tail architecture, which is facilitated through the dimerization arm (Zhang & Cheng, 2003). Multiple studies have demonstrated that naturally occurring mutations (Price et al., 2021), engineered mutations or removal of the dimerization arm impairs dimer formation as well as catalytic activity (Lee et al., 2007; Patounas et al., 2018; Weiss et al., 2000; Zhang et al., 2000; Zhang & Cheng, 2003). These findings emphasize the crucial role dimerization plays in proper PRMT1 function.

Interestingly, numerous reports have observed higher-order PRMT1 oligomers using size-exclusion chromatography, analytical ultracentrifugation (AUC), light scattering methods, and chemical crosslinking; all of which suggest assemblies larger than dimers can exist (Cheng et al., 2011; Feng et al., 2011; Lee et al., 2015; Morales et al., 2015; Toma-Fukai et al., 2016; Troffer-Charlier et al., 2007; Zhang et al., 2000). Additionally, a kinetic study showed that the  $k_{\text{cat}}$  of PRMT1 increases in a concentration-dependent manner (Feng et al., 2011), but a direct correlation to specific oligomeric species was not made. Moreover, it is unclear if higher-order oligomerization occurs at physiological conditions, and despite accumulating evidence that oligomerization may affect activity, a systematic study of the relationship between PRMT1 oligomeric state and methyltransferase activity has never been conducted. In this study, we sought to clarify how oligomerization of PRMT1 proceeds under physiological concentrations, and correlate specific methyltransferase activity with specific oligomers.

Using concentrations of PRMT1 in single human cells determined by quantitative Western analysis and literature values, we defined a window of physiologically relevant PRMT1 concentrations for cultured human cells in the low nanomolar to ~3  $\mu\text{M}$  range. Isothermal spectral shift analysis was used to study oligomerization within that protein concentration window, identifying a model in which PRMT1 exists as monomers, dimers, and tetramers. AUC, Native polyacrylamide gel electrophoresis (PAGE), and PRMT1 mutants displaying different oligomeric states were used to confirm the oligomerization model and to probe the importance of the disordered PRMT1 N-terminus in oligomerization and the effect of active site mutations on oligomerization. A kinetic study correlated specific oligomers with methyltransferase activity. Our results show that the predominant

oligomeric species of WT PRMT1 expected in cells are monomers, dimers, and tetramers. Our results suggest that while dimeric PRMT1 is active with many of the substrates tested, changes in the catalytic efficiency between dimers and tetramers with some substrates, and differential methylation of some substrates by PRMT1 dimers and tetramers could influence the methylarginine proteome.

## 2 | RESULTS

### 2.1 | Physiological concentrations of hPRMT1

In order to understand which PRMT1 oligomeric species are physiologically relevant, it is important to identify the concentration of PRMT1 in individual cells. A previous study used guanidium hydrochloride solubilization and mass spectrometry identification to assess the concentration of PRMT1 in a single HeLa cell at 756 nM (Hein et al., 2015). Although PRMT1 protein expression appears ubiquitous across different types of tissues, quantitative differences in RNA expression and qualitative differences in protein expression have been noted (Anon Human Protein Atlas, n.d.). In order to determine how concentrations of PRMT1 varied over a set of human cell lines we conducted quantitative western blotting of RIPA-solubilized proteins to determine the endogenous concentration of human PRMT1 in four mammalian cell lines. We chose human lung carcinoma cells (A549) due to previous research that identified lung tissue as a major source of asymmetric dimethylarginine, one of the downstream products of PRMT1 (Bulau et al., 2007). Additionally, we included rhabdomyosarcoma (RD) and human cervix carcinoma cells (HeLa) in our analysis since PRMT1 has been shown to be highly involved in their cell differentiation and cell-cycle regulation, respectively (Gao et al., 2010; Goulet et al., 2007). The use of HeLa cells in the western analysis allows for a comparison to previously reported results (Hein et al., 2015). Human embryonic kidney (HEK 293T17) cells were included in the analysis because of their popularity in transfection experiments. Triplicate samples of cell lysates were prepared and immunoblotted alongside recombinant WT PRMT1 standards (Figure S1a). Goulet et al. have previously reported that alternative splicing of the human PRMT1 primary transcript can produce up to seven distinct PRMT1 isoforms that differ at the N-terminus (Goulet et al., 2007). Although the seven variants are expressed differently between human tissues, isoforms 1–3 constitute the majority of PRMT1 in cells and are present in all tissues they tested. Two antibodies which recognize all splice variants at either the carboxy-terminus

epitope (Cell Signaling 2453) or the N-terminus (Cell Signaling 2449) and which have previously been validated in a collection of cell lines (Dashti et al., 2023; Liu et al., 2023; Yao et al., 2021; Zhu et al., 2022) were used for PRMT1 detection. A standard curve created using recombinant PRMT1 allows for a correlation between band intensities and the amount of PRMT1 in the cell samples which, along with cell type specific estimates of cellular volume, was used to calculate cellular concentrations for the selected cell lines (Figure S1). We determined the physiological concentrations of PRMT1 in a single cell to be  $180 \pm 31$  nM in RD,  $94 \pm 51$  nM in HEK 293,  $49 \pm 16$  nM in HeLa, and  $220 \pm 130$  nM in A549 (Figure S1). Our data indicate that PRMT1 expression is uniquely regulated in different cultured cell types with concentrations of RIPA-soluble PRMT1 being submicromolar. Keeping in mind the different solubilization agents and our results with different cell lines, as well as a general 3-fold range in tissue-specific protein expression (Anon Human Protein Atlas, n.d.; Kim et al., 2014; Uhlén et al., 2015), a generous range of low nM to 3  $\mu$ M of PRMT1 was targeted as a proposed physiological range.

### 2.2 | Modeling PRMT1 oligomerization

In order to understand how PRMT1 might oligomerize over physiological protein concentrations, we performed isothermal spectral shift analysis to probe self-association. Spectral shift studies show an  $EC_{50}$  for WT PRMT1 at  $17.9 \pm 5.0$  nM (Figure 1a) that could represent a monomer–dimer, dimer–tetramer, or a monomer–dimer–tetramer equilibrium. Bujalowski and Lohman (1991) reported on using the transition breadth of binding isotherms to distinguish between monomer–dimer (theoretical breadth of 2.86) and monomer–tetramer transitions (theoretical breadth of 1.59), and how the transition breadth can report on the maximum relative population of dimer intermediates. Using this diagnostic (Figure S2), the PRMT1 isotherm shows a breadth of 1.9, which would be most consistent with a monomer–tetramer transition with a maximum of  $\sim 20\%$  of the protein populating dimer intermediates (Figure 1b). These data suggest that monomeric, dimeric, and tetrameric forms of PRMT1 could exist at cellular protein concentrations.

### 2.3 | Low micromolar concentrations of PRMT1 exist as tetramers in solution

The binding data are consistent with a monomer-to-tetramer equilibrium with dimeric intermediates.

However, larger oligomers (e.g., octamers) have also been observed in gel filtration, AUC, cross-linking and small-angle x-ray scattering (SAXS)-based studies (Feng et al., 2011; Mateus et al., 2013; Morales et al., 2015; Toma-Fukai et al., 2016). We therefore sought to directly confirm which oligomeric species of PRMT1 exist in solution at physiological PRMT1 protein concentrations.

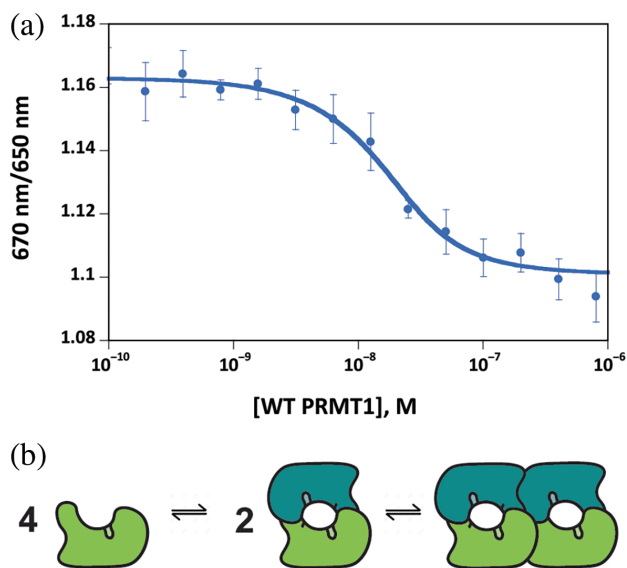


**FIGURE 1** Binding study to monitor PRMT1 oligomerization. (a) The binding isotherm for wild type (WT) PRMT1 (blue) fits to an  $EC_{50}$  of  $17.9 \pm 5.0$  nM. (b) The oligomerization model for PRMT1 at cellular protein concentrations.

For determining the oligomeric state in solution, we performed sedimentation velocity (SV) experiments by AUC. Samples were run either with or without the reducing agent dithiothreitol (DTT) to assess if the formation of oligomers is influenced by reversible oxidative damage (Morales et al., 2015) or disulfide formation (Zhang & Cheng, 2003). At a protein concentration of  $3 \mu\text{M}$ , WT PRMT1 showed a major peak with a sedimentation coefficient of  $8.80 \pm 0.090$  Svedberg (S) (Figure 2, left). The sedimentation coefficient corresponds to a molar mass of 176 kDa which is most consistent with a tetrameric species of PRMT1 (each monomer is 43.5 kDa). The SV profile of WT also showed a very small peak around sedimentation coefficient 2.6 S. It is possible that this is PRMT1 that has undergone cysteine oxidation to sulfenic or sulfonic acid (both of which are unable to be reduced by DTT) and cannot oligomerize. Consistent with this hypothesis, the presence of a reducing agent had no effect on the oligomerization of WT PRMT1. Additionally, a redox-insensitive PRMT1 construct where all 8 surface cysteine residues have been mutated to serine residues (Octamut) (Morales et al., 2015) did not show the monomeric species (Figure 2, right). Finally, the redox-insensitive PRMT1 construct still forms tetramers indicates that disulfides are not used to form the tetramer. Together the data show that PRMT1 is predominantly a tetramer in solution at  $3 \mu\text{M}$ .

Although AUC is the gold standard for determining species distribution in a solution while additionally supporting molecular weight assignment for each detected

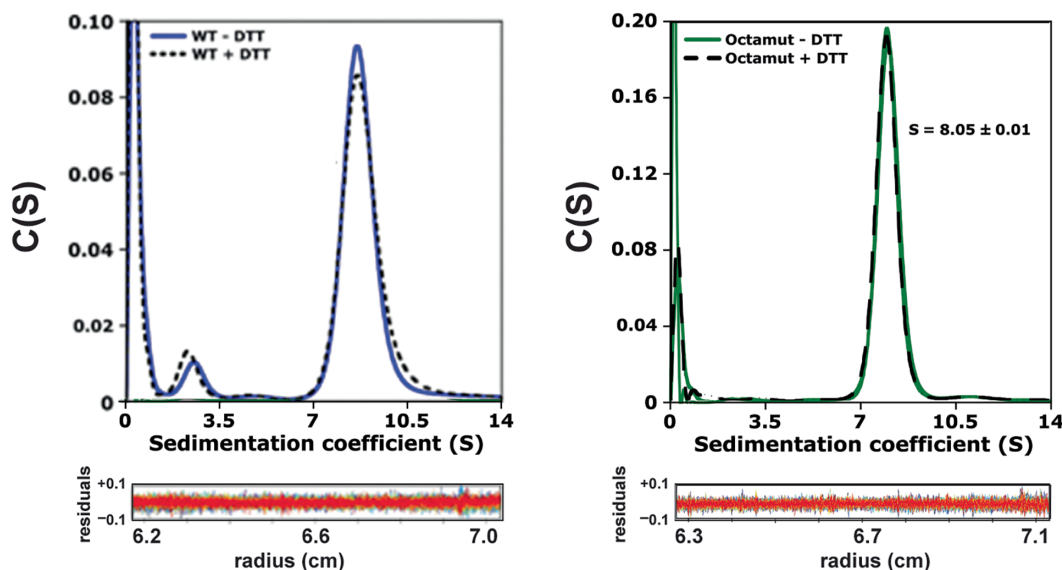


**FIGURE 2** Analytical ultracentrifugation studies show a predominant tetrameric species for low micromolar concentrations of PRMT1. Sedimentation velocity (SV) distribution ( $C(S)$  vs.  $S$ ) plots for PRMT1 (left) and a redox-insensitive PRMT1 (Octamut) (right). Sedimentation profiles with (solid blue) and without (dotted black) 2 mM dithiothreitol (DTT). All SV experiments were run in triplicate at  $3 \mu\text{M}$  protein concentration. Residuals of data plotted against radial location in the cell are located below sedimentation profiles. WT, wild type.



species (Edwards et al., 2020), the AUC instrument used has an optical detection limit preventing analysis of samples with lower protein concentrations. Therefore, to extend our findings to PRMT1 concentrations that are more physiologically relevant, we wanted to implement Native PAGE to analyze the oligomeric state of PRMT1. However, because proteins do not migrate solely based on molecular weight in Native PAGE, we needed to be able to validate the identity of the observed bands. To this end, we sought to identify oligomeric PRMT1 standards for the monomeric, dimeric, and tetrameric species.

## 2.4 | Oligomeric state PRMT1 standards

Toma-Fukai et al. (2016) created a construct of PRMT8 containing three mutations at the tetramer interface predicted to be involved in oligomerization and showed by size-exclusion chromatography (SEC)-SAXS and AUC and that the mutations caused complete dissociation of PRMT8 into a dimer; analogous mutations in PRMT1 also yielded a dimer. Based on these previous studies we created a PRMT1 tetramer interface mutant (TIM) (Y262A/Y304A/L341A) (Figure 3a) to act as our dimer standard. We rationalized that we could also use a PRMT1 construct harboring three mutations in the dimer interface (W197L/Y202N/M206V) (Figure 3a), which we most recently characterized as a monomer (Price et al., 2021). To confirm the oligomeric species of all three PRMT1 constructs at 3  $\mu$ M, we conducted SV experiments. The sedimentation coefficients for the predominant peaks are 2.25S, 3.60S, and 7.08S, corresponding to monomer, dimer, and tetramer (Figure 3b). Using these oligomeric PRMT1 standards characterized by AUC at 3  $\mu$ M, we could then confirm the oligomeric state of the constructs in Native PAGE. For example, WT-PRMT1 (tetramer) was visible by both oriole staining and western blotting and migrated as a tetramer at concentrations from 3  $\mu$ M to 750 nM (Figure 3c).

## 2.5 | Oligomeric state of PRMT1 at submicromolar concentrations

Using the validated PRMT1 oligomeric state standards and Native PAGE with western detection, we evaluated the oligomeric state of PRMT1 at concentrations ranging from 12 to 750 nM. Our results show that the majority of PRMT1 at nearly all concentrations tested exists as a tetramer, with a small amount present as dimer (Figure 4a). The data indicate that in vitro, PRMT1 dimers and tetramers exist at physiological protein concentrations.

The presence of tetrameric PRMT1 at concentrations below 100 nM was a surprise, given that Thomas et al.

(2010) used an m-citrine/m-cerulean PRMT1 pair and fluorescence resonance energy transfer (FRET) to determine a  $K_d$  for dimerization of PRMT1 of  $\sim$ 100 nM. In the FRET study, the observed FRET signal was modeled to dimeric, trimeric, and tetrameric species, with the observed signal most consistent with a dimeric species. If the fluorophores were too far apart in the tetrameric complex, it is possible that the observed energy transfer efficiencies would mimic a dimeric model. The N-terminus is not resolved in many PRMT crystal structures, making it unclear where exactly it resides in solution. In order to understand our results in the context of the FRET study, we determined the oligomeric state of m-citrine PRMT1 by AUC (Figure 4b) and Native PAGE (Figure 4c). At 3  $\mu$ M, the m-citrine PRMT1 is a tetramer, not a dimer. Even at lower concentrations, the tetrameric species is visible in Native PAGE (Figures 4c and S3). Overall the data show that PRMT1 predominantly forms tetramers in solution at low micromolar protein concentrations.

## 2.6 | The disordered N-terminus of PRMT1 is not necessary for tetramer formation

Differential RNA splicing of PRMT1 can lead to PRMT1 proteins that differ in the length of the disordered N-terminus. Additionally, a previous study suggested that the N-terminus of the yeast form of PRMT1 (Hmt1) is involved in regulating the oligomeric state of the enzyme (Messier et al., 2013). To determine if the length of the disordered N-terminus of PRMT1 affects oligomerization we characterized two N-terminal truncations of PRMT1 (S14, which lacks the first 13 amino acids and E27, which lacks the first 26 amino acids) by Native PAGE. As shown in Figure 5, the truncated PRMT1 constructs migrated similarly to full length PRMT1, wherein the predominant species at 500 nM is still a tetramer. These results show that at physiological concentrations of PRMT1, the disordered N-terminus is not necessary for tetramer formation.

## 2.7 | Oligomeric state of PRMT1 loss-of-activity variant at physiological concentrations

Two constructs that are commonly used to express inactive PRMT1 in mammalian cell culture experiments both harbor triple mutations in the AdoMet binding site; the SGT construct involves a triple Ala substitution at residues 69–71 (Balint et al., 2005) and the VLD construct harbors a triple Ala substitution at residues 63–65 (Wada

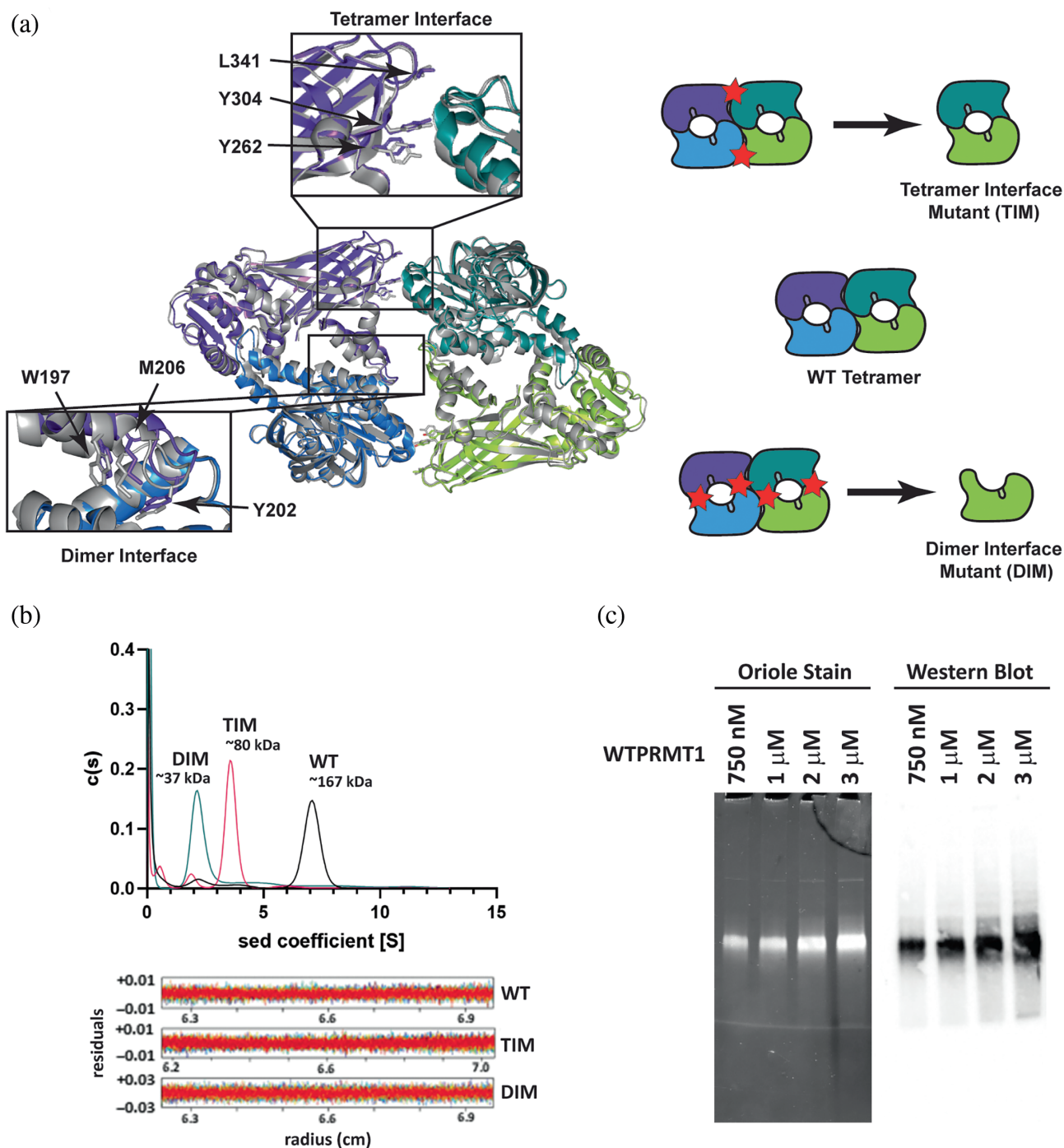


**FIGURE 3** Design and evaluation of PRMT1 oligomeric state standards. (a) Modeled tetrameric unit of PRMT1 created from the octamer structure of PRMT8 (PDB ID 5DST). A dimeric PRMT1 was created using Y262A, Y304A, and L341A mutations. Monomeric PRMT1 was created using W197L Y202N, and M206V mutations. (b) Sedimentation velocity distribution of the various PRMT1 constructs (3  $\mu$ M) by analytical ultracentrifugation (AUC). Residuals plotted against radial location in the cell are below the sedimentation velocity profiles. The sedimentation coefficients for the predominant peaks are 2.25S, 3.60S, and 7.08S, corresponding to monomer, dimer and tetramer. Note, protein samples shown in this figure were dialyzed in buffer containing glycerol which altered the sedimentation coefficient of wild-type (WT) protein compared with what was observed in Figure 2. (c) Various concentrations of WT-PRMT1 were run on Native polyacrylamide gel electrophoresis (PAGE). Proteins were detected using either Oriole fluorescent stain or western blotting.

et al., 2002). Notes in the literature suggest these variants are poorly expressed in mammalian cells (Herrmann & Fackelmayer, 2009), and are observed to be highly

enriched in the nucleus compared with WT (Herrmann & Fackelmayer, 2009). Although these sets of mutations are not directly in the dimer interface, we

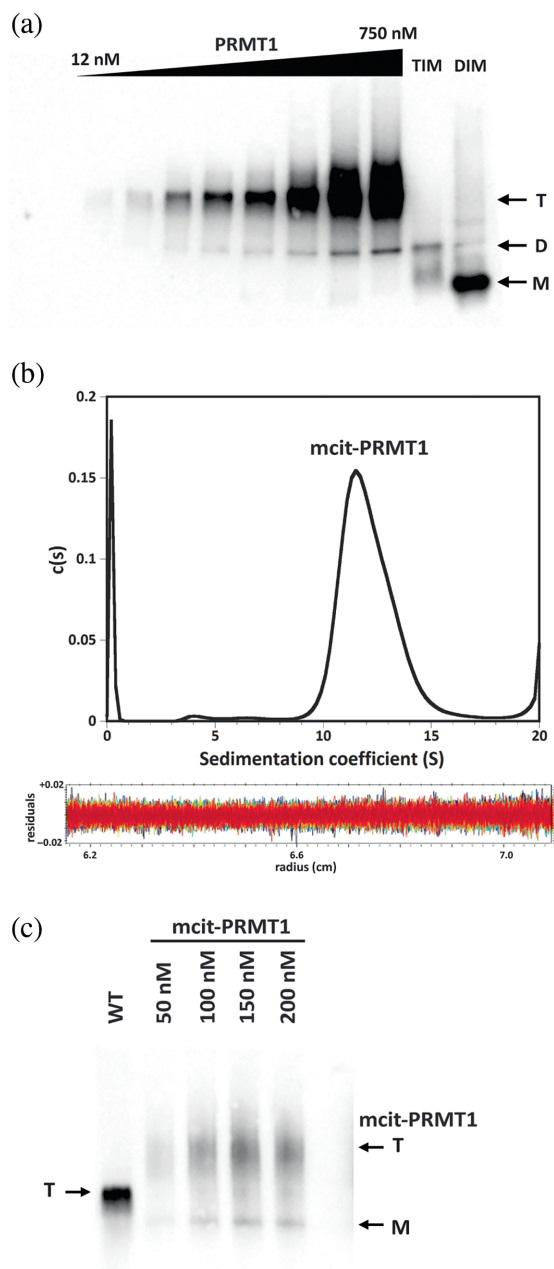


**FIGURE 4** Native polyacrylamide gel electrophoresis (PAGE) analysis shows tetrameric and dimeric PRMT1 predominate *in vitro* at physiological concentrations. (a) Immunoblot of wild-type (WT) PRMT1 run on a 4%–20% Native PAGE at concentrations ranging from 12 to 750 nM. The PRMT1 constructs tetramer interface mutant (TIM, 262A/Y304A/L341A, dimer) and dimer interface mutant (DIM, W197L/Y202N/M206V, monomer) were included as oligomer protein standards. (b) Sedimentation velocity distribution of m-citrine PRMT1 (5  $\mu$ M) by analytical ultracentrifugation. Residuals plotted against radial location in the cell are below the Sedimentation velocity (SV) profile. The sedimentation coefficient for the predominant peak is  $12.07 \pm 0.08$  S, corresponding to 335 kDa (theoretical tetramer 285 kDa). (c) Native PAGE of m-citrine PRMT1 as a function of protein concentration with western blot detection. Oligomer identity is labeled M (monomer) and T (tetramer).

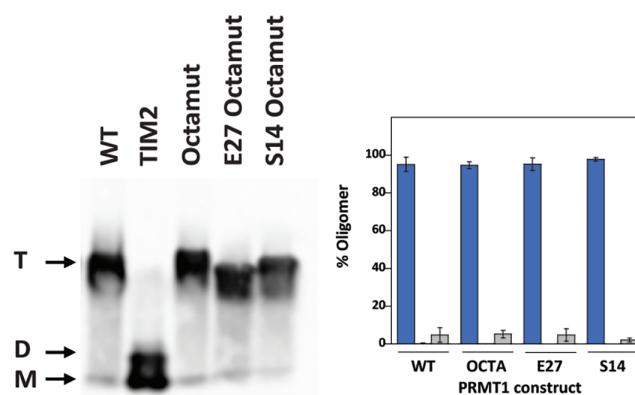


**FIGURE 5** The disordered N-terminus of PRMT1 is not necessary for tetramer formation. The redoxinsensitive full length PRMT1 (Octamut) and truncated versions (S14 and E27) were run on Native polyacrylamide gel electrophoresis to assess oligomer formation using western blot detection. Oligomer identity is labeled M (monomer), D (dimer), and T (tetramer). Quantification of tetramer (blue) and monomer (gray) band intensity is shown in the bar graph. WT, wild type.

questioned whether a collapse of the area due to the smaller residue substitution or the absence of the threonine residue which is near the dimer interface may alter oligomerization. The oligomeric state of SGT PRMT1 was monitored using Native PAGE (Figure 6a). Compared with the WT protein, a significant amount of the SGT PRMT1 protein migrates as a monomeric species. As an alternative, we expressed the previously characterized H293A variant of PRMT1 which shows a 256-fold loss in catalytic efficiency (Rust et al., 2011) and we combined this mutation with the loss of the active site glutamate E153, which shows a 190-fold loss in catalytic efficiency (Rust et al., 2011), creating the H293A/E153A (HE) double variant of PRMT1. Both the H293A and the HE constructs expressed well in bacterial cells, purified similarly to wild-type (WT) enzyme, and migrated in Native PAGE as tetramers at physiological concentrations (Figure 6b). We also confirmed that the HE variant was inactive (Figure S4). Our results show that the SGT triple mutation (and perhaps the VLD triple mutation) affect the ability of PRMT1 to form either dimers/tetramers, suggesting that any PRMT1-dependent scaffolding (Lei et al., 2009) that requires the oligomers would also be impaired with this specific variant as well as the cellular location (Herrmann & Fackelmayer, 2009). Our data suggest the HE variant of PRMT1 may be a better construct to use in mammalian studies that require the use of a methyltransferase inactive variant of PRMT1. Overall, the data show that mutations outside of the dimer and tetramer interface can influence oligomerization of PRMT1 and should be considered as part of mutational analysis.

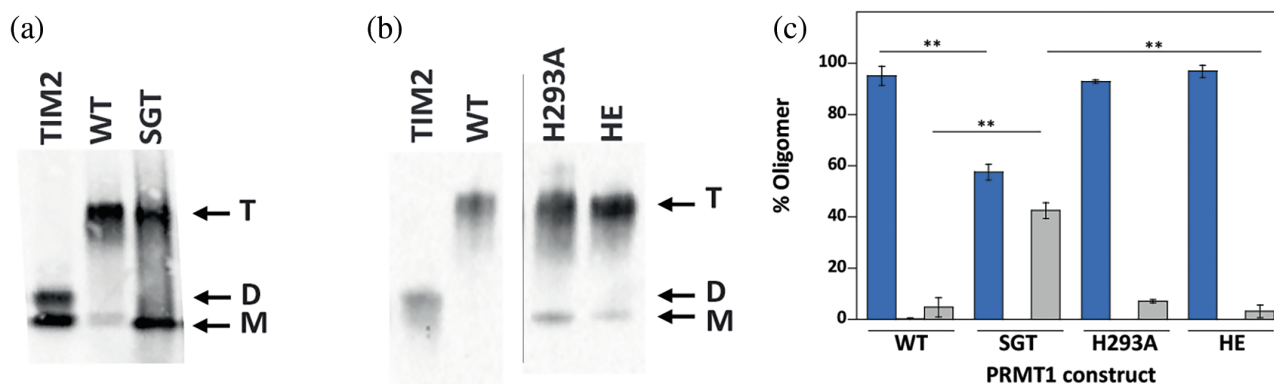


**FIGURE 6** PRMT1 oligomerization can be affected by active site mutations. Native polyacrylamide gel electrophoresis analysis with western blot detection of (a) inactive SGT PRMT1 and (b) the impaired H293A PRMT1 and inactive H293A/E153A. Oligomer identity is labeled M (monomer), D (dimer), and T (tetramer). The vertical line represents where the blot was cut. In (c), band intensity of the tetramer (blue) and the monomer (gray) species were quantified. \*\* $p < 0.01$ , one-way analysis of variance.

## 2.8 | Methyltransferase activity of dimeric and tetrameric species of PRMT1

Our data show that different PRMT1 oligomeric forms, up to and including tetrameric PRMT1, could be present in cells. To better understand how oligomeric state affects activity, we measured methyltransferase activity of WT PRMT1 (tetramer) and the mutant dimeric PRMT1 (TIM). To minimize effects unrelated to oligomerization, we created an additional dimeric variant of PRMT1 (TIM2) using three entirely different mutations at the tetramer interface (Figure S5). Activity of WT and the TIM dimer were assayed at 100 nM using saturating concentrations of R3 peptide as a substrate (Figure 7a). Interestingly, WT (tetramer) and the TIM dimer display activity with this fibrillar peptide substrate, as well as with the protein substrate hnRNPk (Figure 7b). This was a surprising result since Toma-Fukai et al. (2016) noted that dimeric PRMT1 (TIM) was inactive with GST-EWS (RGG3) as a substrate. In order to clarify the discrepancy, we assayed both WT (tetramer) and TIM (dimer) PRMT1 using GST-EWS (RGG3) as a substrate. With the EWS substrate, we observed activity with both the tetrameric and the dimeric PRMT1 (Figure 7c). One explanation as to why we obtained contradictory results may reside in different assay conditions and the stability of the dimeric PRMT1. Previously the dimeric PRMT1 mutant was assayed over an hour-long incubation with GST-EWS (RGG3) as a substrate using a gel assay (Toma-Fukai et al., 2016). On the other hand, the current study employed a more sensitive assay requiring <10 min to yield a linear rate (Hevel & Price, 2020; Suh-Lailam & Hevel, 2010). This suggests that stability may be different between the dimer and tetramer forms of PRMT1, but clearly shows that dimeric PRMT1 is a functional methyltransferase.

Contrary to previous reports (Toma-Fukai et al., 2016), our studies clearly show that both the tetrameric and dimeric forms of PRMT1 are active. Although both AUC and Native PAGE show that the tetramer interface mutants (TIM and TIM2) of PRMT1 behave as dimeric proteins in solution, we cannot exclude the possibility that the TIM mutants form tetramers in the presence of peptide or protein substrates, or that the tetrameric species dissociates to a dimer in the presence of substrate. To address this possibility, we questioned if we could capture the PRMT1 oligomers bound to substrate through glutaraldehyde crosslinking. Figure 8 shows that with an H4 peptide substrate, a high-molecular weight cross-linked species is observed in reactions containing WT tetrameric PRMT1, that is barely visible when the dimeric PRMT1 variant is used. The data indicate that the dimeric PRMT1 and monomeric variants can bind peptide substrates and that the presence of peptide substrate does not induce tetramer formation.

## 2.9 | Activity as a function of equilibrating oligomeric PRMT1 species

In order to understand how activity is regulated as a function of a *specific* oligomeric state, we determined the  $k_{cat,app}$  of both WT PRMT1 and a TIM2 as a function of protein concentration (Figure 9) with the H421 peptide as a substrate, and correlated this with our model of oligomerization (Figure 1b). Our results with WT PRMT1 look similar to those of Feng et al., albeit  $k_{cat,app}$  saturates at lower protein concentration in our study. The concentration of WT PRMT1 promoting the half maximal  $k_{cat,app}$  is  $10 \pm 1$  nM. Based on the  $EC_{50,tetramerization}$  of  $\sim 18$  nM measured in Figure 1a, the change in  $k_{cat}$  is



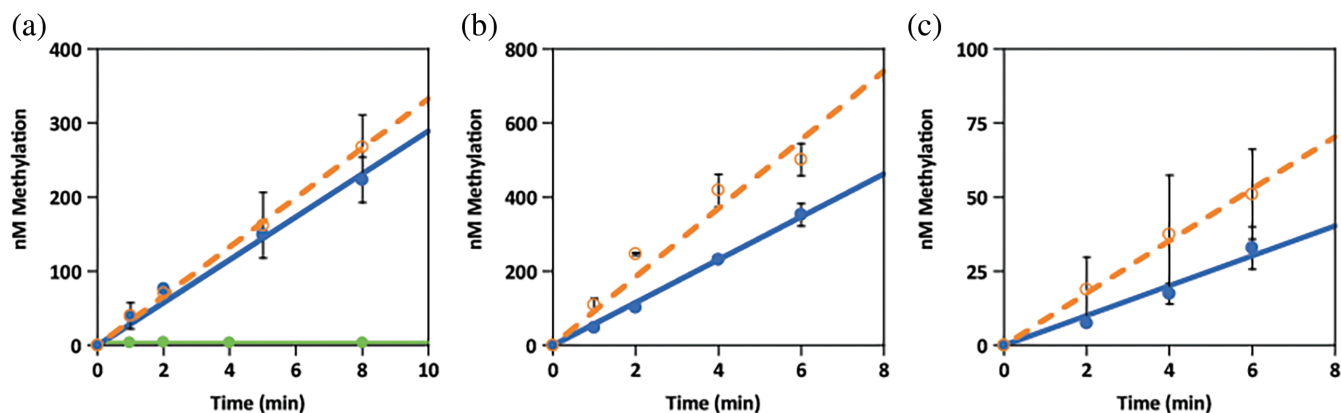
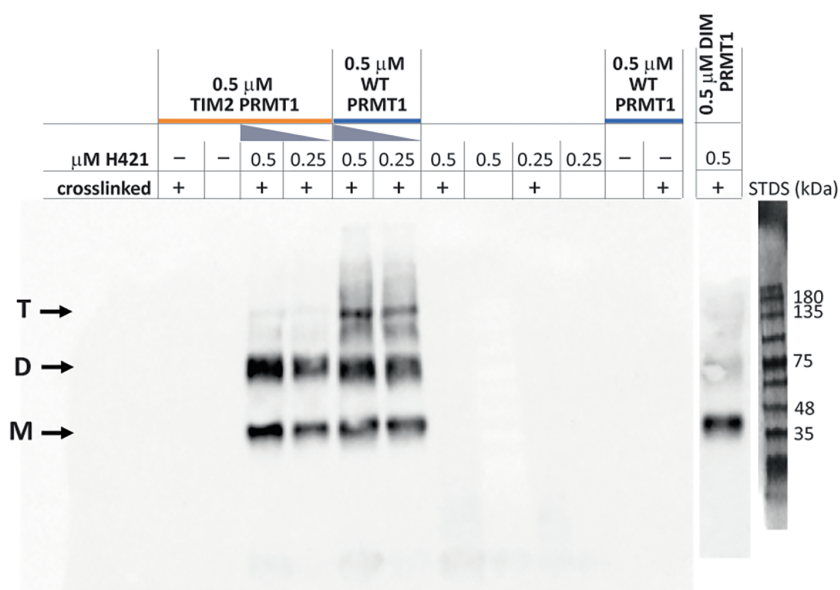


**FIGURE 7** Methylation activity assays of wild-type (WT) PRMT1 (tetramer), tetramer interface mutant (TIM) PRMT1 (dimer), and dimer interface mutant (DIM, monomer). Methyltransferase activity of 100 nM WT PRMT1 (blue closed circles, solid line), TIM-PRMT1 (open orange circles, dashed line), or DIM (green circles) using 2 μM AdoMet and (a) 200 μM R3 peptide, (b) 4 μM hnRNPK protein, (c) 4 μM GST-EWS substrates.

**FIGURE 8** Cross-linking of peptide substrate to wild-type (WT) PRMT1 (tetramer), tetramer interface mutant (TIM)2 PRMT1 (dimer), and dimer interface mutant (DIM) PRMT1 (monomer). The biotinylated H421 peptide substrate was crosslinked to WT, TIM2, or DIM PRMT1 using glutaraldehyde and samples were separated using sodium dodecyl sulfate-polyacrylamide gel electrophoresis and transferred to polyvinylidene difluoride. The blot was probed for biotin using StrepTactin-HRP. Protein standards (STDS) were imaged colorimetrically.



consistent with a monomer/dimer/tetramer transition wherein both dimer and tetramer have full or near full activity with H421 peptide and monomer is inactive. The tetramer interface variant (TIM2) kinetic data fits to a simple hyperbolic curve with an  $EC_{50}$  of  $44.3 \pm 8.0$  nM, which agrees well with the  $K_{d,dimerization}$  of  $\sim 48$  nM measured by isothermal spectral shift (Figure S6).

## 2.10 | Oligomerization affects catalysis in a substrate-dependent manner

Although the H421 peptide was methylated equally well by the tetrameric and dimeric forms of PRMT1, the initial data suggested that some substrates may be differentially methylated by one oligomer versus the other. In order to

test if the tetrameric and dimeric forms of PRMT1 have different catalytic specificities, we further characterized both WT (tetramer) PRMT1 and TIM2 (dimer) PRMT1 with the protein substrate hnRNPA1 (Figure 10a). The apparent  $k_{cat}/K_m$  values for tetramer and dimer were  $0.14 \pm 0.04$  and  $0.24 \pm 0.03 \text{ min}^{-1} \mu\text{M}^{-1}$ , respectively. These data suggest that changes in the oligomeric state of PRMT1 could impact how well specific substrates are methylated.

In most cases, the dimeric variant of PRMT1 demonstrated equal or more activity than the WT tetrameric version of PRMT1 for the substrates we tested. However, we hypothesized that there may be some substrates that are preferentially methylated by the tetramer. We noted a study in the literature (Lee et al., 2015) that created a chimeric PRMT8 construct by swapping out a small



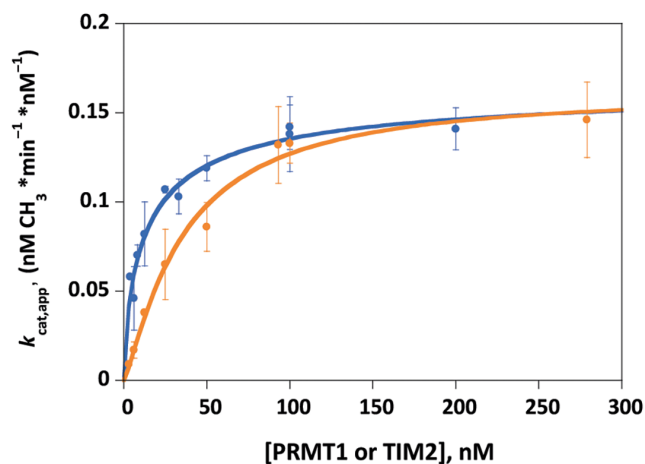


**FIGURE 9** Kinetic characterization of wild type (WT) and tetramer interface mutant (TIM)2 PRMT1 with H421 as a substrate.  $k_{cat,app}$  of WT PRMT1 (blue) and the TIM2 PRMT1 construct (orange) as a function of PRMT1 protein substrate concentration. Activity was measured using 20  $\mu\text{M}$  H421 peptide substrate in the presence of 10  $\mu\text{M}$  AdoMet at 30°C.

section of the  $\beta$ -barrel with the same section from yeast PRMT1 (Hmt1). The protein substrate NIFK was methylated by PRMT8 (and PRMT1), but not the chimeric PRMT8. When we examined the AUC profiles for WT and chimeric PRMT8 (performed at 6–9  $\mu\text{M}$ ), the predominant peak in the profile is a tetramer, but the chimeric protein also exhibits species consistent with dimer and/or monomer. Mapped onto the PRMT1 structure (Figure S7), the small swap included a loop in the tetramer interface. This suggested to us that the PRMT8 chimeric swap could have altered the  $K_d$  for tetramerization in the chimeric PRMT8 variant and at concentrations used to measure methyltransferase activity, perhaps the chimeric variant was a dimer in the kinetic assay. Based on this we used both WT PRMT1 and dimeric TIM and TIM2 PRMT1 to try and methylate NIFK. As Figure 10b shows, only the tetrameric WT PRMT1 could methylate NIFK. Our data show that the oligomeric state of PRMT1 can affect the catalytic efficiency of PRMT1 as well as substrate selection.

### 3 | DISCUSSION

#### 3.1 | Physiologically relevant PRMT1 oligomers

Given the nM dissociation constant for PRMT1 and the nanomolar to low micromolar concentrations of PRMT1 in cells, it would seem that the dimeric and tetrameric forms of PRMT1 will predominate in many cell types.

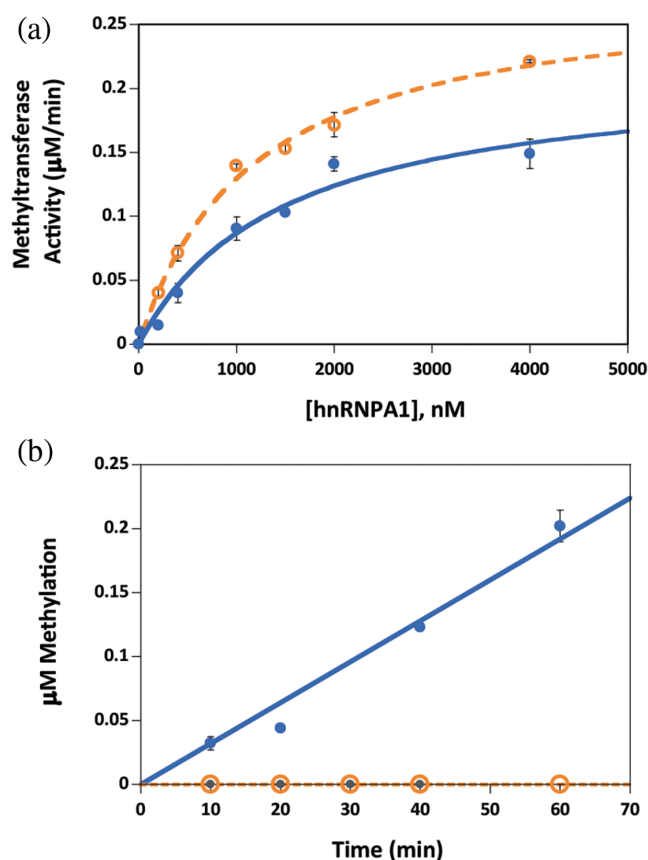


**FIGURE 10** Oligomeric state of PRMT1 can affect the catalytic efficiency of PRMT1 as well as substrate selection. (a) Activity of wild-type (WT) PRMT1 (closed blue circles, solid line) and the tetramer interface mutant (TIM)2 PRMT1 construct (open orange circles, dashed line) as a function of hnRNPA1 protein substrate concentration. (b) Activity of tetrameric WT PRMT1 (closed blue circles, solid line) and the dimeric PRMT1 constructs (TIM2, open orange circles, TIM, closed black circles, dashed lines) as a function of time using 4  $\mu\text{M}$  NIFK protein as a substrate.

Cells expressing very low amounts of PRMT1 (Su et al., 2019) might be expected to harbor inactive, monomeric PRMT1; however, even small changes in protein expression in these cells would “turn on” methyltransferase activity of PRMT1 by promoting dimerization. Several studies have noted upregulation of PRMT1 protein expression under a variety of conditions (Jia et al., 2023; Liu et al., 2016; Park et al., 2021). A survey of the data suggests perhaps a 3-fold increase in PRMT1 concentration may be feasible, bringing the concentration to an estimated 9  $\mu\text{M}$  where additional oligomers may be present. Indeed, the fit for the lower portion of the binding isotherm for WT PRMT1 suggests that there could be another species above 4  $\mu\text{M}$  that we could not capture due to limits of protein solubility in the experiment. However, one must also consider that the guanidinium hydrochloride solubilization method captures mobile and

immobilized fractions of PRMT1 (Maxwell et al., 2003). Given that the RIPA-solubilization method resulted in lower PRMT1 protein concentrations, it suggests that, at least in HeLa cells, a portion of the PRMT1 is tied up in immobilized fractions and would not be available as part of the equilibrating pool. Additionally, interaction of PRMT1 with partner proteins (substrates and regulators) and AdoMet or AdoHcy (Thomas et al., 2010; Toma-Fukai et al., 2016; Zhou et al., 2015) *in vivo* would also have the potential to perturb the oligomerization equilibrium.

In addition to PRMT1 protein concentration and protein interactions, naturally occurring mutations and post-translational modifications could affect the oligomeric state of PRMT1 in cells. A review of the COSMIC database (Anon cancer.sanger.ac.uk/cosmic, n.d.; Tate et al., 2019) identified several mutations that exist in or near the tetramer interface (Figure S8), and our lab previously characterized naturally occurring dimer interface mutants (DIM) that behave as monomers in solution (Price et al., 2021). In addition to single-site mutants, splice variants lacking exons 8/9 that encode the dimerization arm have been identified that likely do not form dimeric species (Adamopoulos et al., 2019; Patounas et al., 2018). Importantly, in at least one case the variant correlates with cellular malignancy (Patounas et al., 2018). Likewise, mass spectrometry studies (Hornbeck et al., 2015) of PRMT1 have revealed several sites of lysine ubiquitinylation, acetylation, and succinylation that may be expected to alter oligomerization of PRMT1 (Figure S9). Collectively the data show that monomer, dimers and tetramers are relevant at cellular PRMT1 concentrations.

### 3.2 | Consequences of PRMT1 oligomerization

The PRMT field has widely agreed that most PRMTs must *at least* form a dimer to perform catalysis (Patounas et al., 2018; Price et al., 2021; Zhang & Cheng, 2003; Zhou et al., 2015). The results presented in this study are consistent with monomeric PRMT1 being inactive. What has become confusing is whether or not the dimer is *sufficient* for activity and what if anything happens after dimer formation under physiological conditions. Our results clearly show that dimeric PRMT1 displays methyltransferase activity, indicating that the dimer is indeed the minimal unit necessary for methyltransferase activity. This means that studies done at very low concentrations of PRMT1 (below the  $K_d$ ) could demonstrate low to no activity; this is a potential explanation for why the dimeric variant of

PRMT1 was previously characterized as inactive (Toma-Fukai et al., 2016). Alternatively, the dimer of PRMT1 may be less stable than the tetrameric form.

With some substrates such as the R3 peptide and the H421 peptide, the activity of the dimeric and tetrameric PRMT1 is nearly identical. Coupled with the binding isotherms and AUC studies, our data are consistent with explaining the protein-dependent increase in  $k_{cat}$  observed by Feng et al. (2011), with the H421 peptide as due to the dimerization of PRMT1, with tetramerization having no further effect on  $k_{cat}$ . On the other hand, the efficiency of methylating other substrates, such as hnRNPA1 and particularly NIFK, is different between the dimer and tetramer forms of PRMT1. We note that the dimeric PRMT1 species were created using a mutated surface that could also be important for substrate binding; however, the fact that neither mutant (where the mutations exist on different portions of the protomer, Figure S5) could methylate NIFK makes this alternate explanation less likely. This suggests that altering the ratio of dimeric and tetrameric forms of PRMT1 *in vivo* could alter which proteins are more readily methylated.

The ability of proteins to form higher-order oligomers can induce allosteric behavior on the protein (Frieden, 2019). Indeed, allostery in PRMT1 has been investigated by Zhou et al. (2015), but should be reinvestigated in the context of the new PRMT1 oligomerization paradigm. Having oligomeric PRMT1 standards to properly assign the oligomeric state of the mutants and an ability to assess this at the same concentrations used to measure methyltransferase activity is necessary in order to deconvolute if a residue is solely involved in oligomerization or has additional roles in catalysis.

The presence of both dimeric and tetrameric PRMT1 also presents the potential to control interactions of other proteins with PRMT1. Heterooligomerization of PRMTs is gaining interest as a common regulatory mechanism for controlling activity and substrate selection of the PRMTs (Cao et al., 2023; Chen et al., 2023; Herrmann et al., 2009; Hobbie & Schaner Tooley, 2024; Lee et al., 2005; Liu et al., 2022; Pak et al., 2011; Rowley et al., 2023). However, it is unclear if heterooligomerization occurs between dimers composed of the same isoform or tetramers of heterodimers. As protein-protein interaction inhibitors that impair oligomer formation have been documented (Singh, 2018), understanding how PRMT heterooligomers form represents a new avenue to explore therapeutic targeting. In addition to intrafamily interactions, different oligomers of PRMT1 may preferentially bind known regulators or be preferentially modified by enzymes (Hartley & Lu, 2020) or differentially affect scaffolding.

## 4 | CONCLUSIONS

We have defined an oligomerization paradigm for PRMT1 and show that the biophysical characteristics of PRMT1 are poised to support a monomer/dimer/tetramer equilibrium in vivo. We further show that the oligomeric state of PRMT1 can affect the catalytic efficiency of PRMT1 as well as substrate selection.

## 5 | MATERIALS AND METHODS

### 5.1 | Reagents

[<sup>3</sup>H-methyl] S-adenosyl-methionine (AdoMet) (83.1 Ci/mmol) was bought from Perkin Elmer, and nonradioactive AdoMet was bought from Sigma as a chloride salt (≥80%, from yeast). ABclonal synthesized the R3 peptide (Acetyl-GGRGGFGGRGGFGGRGGFGGK, biotin conjugated to C-terminal lysine) and the H421 peptide (Acetyl-SGRGKGGKGLGKGGAKRHRKVGK, biotin conjugated to C-terminal lysine). ZipTip<sup>®</sup><sub>C4/C18</sub> pipette tips were acquired from Millipore and TGX gels were purchased from Bio-Rad. The pGEX-1 vector encoding Ewing Sarcoma RGG3 (EWS-RGG3) was obtained from Dr. Toma-Fukai (Nara Institute of Science and Technology).

### 5.2 | Plasmid generation

Generation of the WT His<sub>6</sub>-ratPRMT1 (PRMT1) plasmid was previously described (Morales et al., 2015). The rat PRMT1 DNA sequence was humanized to the human isoform 3 variant 1 of PRMT1 (UniProt ID: Q99873-3) by encoding a single amino acid substitution H161Y. The PRMT1 constructs W197L/Y202N/M206V (DIM), and Y262A/Y304A/L341A (TIM) each in a pET28b vector containing a His<sub>6</sub>-tag and tobacco etch virus (TEV) cleavage site were synthesized by General Biosystems. The PRMT1 construct H64A/R66A/H278A (TIM2) was cloned into a pET28b vector also containing a His<sub>6</sub>-tag and TEV cleavage site and was synthesized by Twist Biosciences. The plasmids encoding the H293A and E153A/H293A (HE) PRMT1 constructs were made through site-directed mutagenesis using the pet28b/ His<sub>6</sub>-humanized WT PRMT1 plasmid as a template. The plasmid encoding the SGT79AAA PRMT1 was synthesized by Genscript as an N-terminal Strep fusion and inserted into pET28b at the *Nco*I and *Xho*I sites. The plasmid encoding NIFK (UniProt ID Q9BYG3) (Pan et al., 2015) was synthesized by Genscript.

### 5.3 | Expression and purification of recombinant proteins

*Escherichia coli* BL21 (DE3) cells containing the His<sub>6</sub>-TEV-WT PRMT1 plasmid were grown in Luria Broth at 37°C, induced at OD<sub>600</sub> 0.6–0.8 with 0.2 mM IPTG, and grown an additional 24 h at 25°C. Cell pellets were resuspended in a 1:3 cell mass-to-buffer ratio using Lysis buffer A (50 mM sodium phosphate, 5 mM imidazole, 1 mM ethylenediaminetetraacetic acid (EDTA), 1 mM DTT, pH 7.6). Cells were lysed by sonication and the lysate was clarified by centrifugation. The supernatant was treated with 5% (w/v) solution of 60,000 M<sub>n</sub> Branched polyethylenimine (PEI) (ACROS Organics) dropwise to precipitate nucleic acids, incubated 5–10 min, then re-clarified through centrifugation. The soluble fraction was incubated with loose Ni-NTA resin (GoldBio) with constant agitation for 2–3 h at 4°C. The bulk of impurities were removed by batch washing the resin extensively with Wash Buffer (50 mM sodium phosphate, 1 mM DTT, 0.25 mM EDTA pH 7.6 20 mM imidazole). WT PRMT1 was eluted from the resin using an imidazole gradient. Elution fractions containing WT protein were pooled and dialyzed overnight in 50 mM sodium phosphate, 5% glycerol, 2 mM EDTA, 2 mM DTT pH 7.6. Proteins were concentrated in a 30,000 molecular weight cutoff spin concentrator to ≥3 mg/mL, beaded in liquid nitrogen, and stored at –80°C. Expression and purification of the H293A and HE mutants were similar to that for WT PRMT1. Expression and purification of TIM-PRMT1 and TIM2-PRMT1 was identical to WT-PRMT1 except an additional HiTrap Q HP column (Cytiva) was used after Nickel for both constructs and TIM2 was induced with 0.5 mM IPTG. The DIM construct purification was reported previously (Price et al., 2021). The plasmid encoding fluorescently tagged mcit-PRMT1 was a kind gift from Dr. Adam Frankel (University of British Columbia). The mcit-PRMT1 protein was expressed and purified similarly to the literature (Thomas et al., 2010) with the following modifications. Cells were induced with 0.5 mM IPTG at 16°C overnight. Cells were resuspended in lysis buffer (50 mM Hepes-KOH pH 7.6, 1 M NH<sub>4</sub>Cl, 20 mM imidazole, 1 mM phenylmethanesulfonyl fluoride, 1 mM DTT, 0.1% Tween-20 and Pierce Protease Inhibitor cocktail). The mcit-PRMT1 protein was purified using HisTrap and gel filtration chromatography (Thomas et al., 2010) and stored in 50 mM Hepes-KOH pH 7.6, 2 mM EDTA, 1 mM DTT and 200 mM NaCl. Protein purity was assessed by sodium dodecyl sulfate-polyacrylamide gel electrophoresis (SDS-PAGE; Figure S10) and protein concentrations were determined spectrally using the predicted extinction coefficient for each construct.

Expression and purifications of GST-EWS-RGG3 (a 113 amino acid portion of the EWS protein) (UniProt

ID Q01844; Takahama et al., 2011), and hnRNPK (Uniprot ID P61978; Moritz et al., 2014), and NIFK (Pan et al., 2015) were performed as described previously. The hnRNPA1 protein was expressed and purified as described (Kooshapur et al., 2018) with the following modifications: a 5% PEI treatment step was performed as above, prior to binding the Ni-NTA resin, to lower the amount of nucleic acids bound to the protein. The His tag was not cleaved from the protein.

Plasmid encoding SGT79AAA PRMT1 was transformed into BL21 (DE3) cells, which were grown in Luria Broth at 37°C, induced at OD<sub>600</sub> 1.6–1.8 with 0.2 mM IPTG, and grown an additional 24 h at 16°C. Cells were resuspended in 50 mM sodium phosphate (pH 7.6), 2 mM EDTA, 2 mM DTT, sonicated, and the cell lysate was clarified through centrifugation. Supernatant for SGT was loaded onto a StrepTactin XT 4Flow High-Capacity column and washed with 50 mM sodium phosphate (pH 7.6), 2 mM EDTA, 2 mM DTT, 50 mM D-Biotin, and eluted using 50 mM NaPO<sub>4</sub> (pH 7.6), 2 mM EDTA, 2 mM DTT, 100 mM D-Biotin. Fractions containing SGT SGT79AAA were used directly from the column in Native PAGE experiments.

## 5.4 | Preparing mammalian soluble cell lysates

Mammalian cell lines RD and HEK 293 T/17 were maintained in Dulbecco's Modified Eagle Medium (DMEM) with 10% fetal bovine serum (FBS) (VWR) while HeLa Ohio and A549 cells were grown in MEM 10% FBS (VWR). Cells were incubated at 37°C in the presence of 5% CO<sub>2</sub>. For harvest, cells were detached with 5% w/v Trypsin (Hyclone) before being counted with a hemocytometer to determine total cell count per flask. Cell cultures were pelleted by centrifugation at 823×g at 4°C for 10 min and culture media was carefully removed from the cell pellet. Pellets were frozen with liquid nitrogen and immediately stored at –80°C. Cells were thawed on ice and resuspended in a 1:3 ratio of cell pellet to RIPA buffer (between 60 and 150 μL RIPA) with a protease inhibitor cocktail (Pierce PIA32955), then lysed by freeze–thaw in liquid nitrogen. Benzonase nuclease was added to the cell lysate for DNA degradation and centrifuged at 21,000×g for 45 min at 4°C. Total protein concentration of the supernatant was determined using a DC protein assay (Bio-Rad).

## 5.5 | Quantitative immunoblotting

Western blot analyses were performed using three biological replicates of mammalian cell lysates with recombinant WT His-PRMT1 standards. Two different PRMT1

antibodies were used, one specific to the amino-terminus (Cell Signaling 2449) that recognizes the three major splice variants of PRMT1, and one specific to the carboxy-terminus that recognizes all splice variants (Cell Signaling 2453). Blots were incubated overnight at 4°C with either PRMT1 rabbit α-N-terminus or α-C-terminus polyclonal antibody with constant agitation. Blots were washed twice with Tris-buffered saline with 0.1% Tween 20 (TTBS) and incubated for 1 h at 25°C with mouse α-rabbit-horse radish peroxidase (HRP) conjugated secondary antibody (Cell Signaling 7074). Before imaging, blots were washed thoroughly six times with TTBS. Amersham ECL Prime western substrate (GE Healthcare 2232) was used for imaging. western blot band intensity was quantified with ImageLab 5.1 software, and PRMT1 standard band intensities were plotted as a function of protein input and fit with a linear curve. In order to quantify endogenous PRMT1 concentrations, we found that HeLa cells have an average volume of ~3000 μm (Bulau et al., 2006), and A549 cells have a volume of 1670 μm (Bulau et al., 2006; Jiang et al., 2010; Milo, 2013). HEK 293 T17 cells were previously determined to be relatively spherical in shape and have an approximate radius of 6.95 μm. Using the equation for finding the volume of a sphere we calculated a cell volume of 1406.19 μm<sup>3</sup> for a HEK 293 T17 cell (Mateus et al., 2013). We could not find an estimate for the average volume of an RD cell in the literature, so images of RD cells were compared with HeLa and HEK293T17 cells (images from ATCC) and it was determined that RD cell volume appears to be between that of HeLa and HEK 293 T17, so the approximated RD cell volume is 2200 μm<sup>3</sup>. The total volume of cell lysate was found by multiplying the volume of a single cell by the number of cells in the pellet and added to the amount of RIPA buffer used for resuspending the pellet as shown below, where V refers to volume.

$$\begin{aligned} \text{Total V lysate}(\mu\text{L}) &= [\text{V one cell}(\mu\text{L}) \times \#\text{cells in pellet}] \\ &+ \text{V RIPA buffer}(\mu\text{L}) \end{aligned} \quad (1)$$

Using the western blot standard curve, the amount of PRMT1 in the mammalian gel sample was found in nanograms of PRMT1 per microliter of sample loaded and converted to nanomolar concentration of PRMT1 in the gel. We accounted for the dilution in preparing the SDS sample as shown:

$$\begin{aligned} &[\text{PRMT1}]_{\text{cell lysate}}(\text{nM}) \\ &= \frac{[\text{PRMT1}]_{\text{gel sample}}(\text{nM}) \times \text{total V SDS sample}(\mu\text{L})}{\text{volume of lysate used for SDS sample}(\mu\text{L})} \end{aligned} \quad (2)$$



The concentration of PRMT1 in a single mammalian cell was found using the equation below by taking the total volume of lysate (Equation 1) multiplied by the nanomolar concentration of the lysate (Equation 2) divided by the combined internal volume of mammalian cells.

$$\frac{[\text{PRMT1}] \text{ in one mammalian cell (nM)}}{= \frac{\text{total V lysate } (\mu\text{L}) \times [\text{PRMT1}] \text{ in lysate (nM)}}{\text{combined V of cells in pellet } (\mu\text{L})}} \quad (3)$$

## 5.6 | SV experiments and data analysis

SV experiments were performed in a Beckman Proteome-Lab XL-I analytical ultracentrifuge equipped with scanning optics using an 8-hole rotor, 12 mm carbon-filled epoxy double-sector centerpieces, and quartz windows. Proteins to be analyzed were dialyzed in 50 mM sodium phosphate, 2 mM EDTA,  $\pm 2$  mM DTT, pH 7.6 overnight at 4°C unless stated otherwise. Calculated molecular weights of proteins analyzed were as follows: WT PRMT1 at 43.54 kDa, DIM PRMT1 at 43.38 kDa, TIM and TIM2 PRMT1 at 43.31 kDa. Protein samples (3–7  $\mu\text{M}$ ) were prepared in the same buffer used for dialysis and filtered with a 0.22  $\mu\text{m}$  filter prior to loading into the cell. Prepared cells were placed in the 8-hole rotor, and temperature equilibrated at 20°C while resting under vacuum in the rotor chamber. SV scans were carried out at a rotor speed of 40,000 rpm while recording absorbance at 280 nm. Compete sedimentation was confirmed by following the absorbance of each scan (Figure S9). Buffer density, viscosity, protein partial specific volumes were calculated using the software Sednterp (Lebowitz et al., 2002). All SV data analysis was performed using the program Sedfit (Schuck, 2000). Differential sedimentation coefficient distributions were calculated by least-squares boundary modeling of SV data using the continuous distribution  $c(s)$  Lamm equation model.

## 5.7 | Native PAGE

PRMT1 samples were prepared containing 12–750 nM protein in 50 mM sodium phosphate, 1 mM DTT, 1 mM EDTA, and 5% glycerol at pH 7.6. DIM PRMT1 (W197L/Y202N/M206V) and TIM PRMT1 (Y262A/Y304A/L341A) were included as protein standards for monomeric and dimeric PRMT1, respectively. Samples were mixed and allowed to incubate at 25°C for 15 min then run on a 4%–20% TGX Mini-PROTEAN Precast Protein Gel at 100 V for 10 h at 4°C. We noted that the TIM and TIM2

(dimeric mutants) migrate as a combination of monomers and dimers at concentrations used in Native PAGE, suggesting that the conditions perturb the equilibrium but can nonetheless be used to identify where the monomeric and dimeric species migrate. The loss of activity variant SGT was desalted in a Zeba spin column (Thermo Fisher) prior to loading. For both gels, proteins were transferred to polyvinylidene difluoride (PVDF) and analyzed using the same methods described for immunoblotting.

## 5.8 | Methyltransferase assays of PRMT1 activity

Discontinuous methylation assays were performed as described previously (Hevel & Price, 2020; Su et al., 2019). Reactions contained 100 nM enzyme, 2  $\mu\text{M}$  AdoMet (1  $\mu\text{M}$  [H (Bulau et al., 2006)]AdoMet), 0.38  $\mu\text{M}$  BSA, 10 nM MTAN (5'-methylthioadenosine/S-adenosylhomocysteine nucleosidase), and 1 mM DTT in 50 mM sodium phosphate pH 7.6. Activity was measured at 37°C and initiated with 200  $\mu\text{M}$  R3 peptide or 4  $\mu\text{M}$  protein substrate. At different time points, 5  $\mu\text{L}$  samples of the reaction were quenched in 6  $\mu\text{L}$  of 8 M guanidinium hydrochloride. Samples were processed with Zip-Tip<sub>C18</sub> pipette tips (Millipore) for removal of unreacted [ $\text{H}^3$ ]AdoMet and recovery of the radiolabeled product. Radiolabeled product produced for each time point was quantified by a liquid scintillation counter.

In order to quantify methyltransferase activity over a broad range of enzyme concentrations, 20  $\mu\text{L}$  reactions containing 50 mM Hepes (pH 8.0), 20  $\mu\text{M}$  H4-21 peptide, 10  $\mu\text{M}$  AdoMet (2  $\mu\text{M}$  [ $\text{H}^3$ ]AdoMet and 8  $\mu\text{M}$  unlabeled AdoMet), 1 mM DTT, varied BSA to keep the total protein concentration at 0.48  $\mu\text{M}$  were pre-incubated for 1 min at 30°C, and then were initiated with WT PRMT1 or TIM2 at concentrations ranging from  $\sim 3$  to  $\sim 300$  nM. The unreacted [ $\text{CH}_3\text{—H}^3$ ]-methylated product was separated from unreacted [ $\text{H}^3$ ]AdoMet using ZipTips<sub>C18</sub> as described above. Rates were collected under linear conditions (e.g., 20 min for 3 nM enzyme, 4 min for 300 nM enzyme). The methyltransferase activity between a freshly diluted enzyme sample and a sample that had been pre-diluted and incubated for 30 min was identical, suggesting that oligomer equilibrium at the low enzyme concentrations was reached before the enzyme reaction was initiated.

Alternatively, the full kinetic characterization of hnRNPA1 protein and the measurement of NIFK methylation was accomplished using the commercially available MTase-Glo kit from Promega. Briefly, reactions contained



20 mM Tris-HCl (pH 8.0), 50 mM NaCl, 3 mM MgCl<sub>2</sub>, 1 mM EDTA, 1 mM DTT, 0.1 mg/mL BSA, hnRNPA1 (0–4 μM), and 10 μM AdoMet. Reactions for hnRNPA1 methylation were initiated with 100 nM enzyme and proceeded at 37°C. The methylation of 4 μM NIFK was initiated with 1 μM enzyme and used 50 μM AdoMet. Reaction timepoints were taken and quenched in 0.5% TFA. Timepoints were chosen in the linear range of the reaction. The MTase Glo reagent and MTase Glo Detection reagents were added to each reaction and *S*-adenosyl-L-homocysteine (AdoHcy) standards following the manufacturer's protocol. Luminescence was detected with a BioTek luminometer; relative luminescence was converted to AdoHcy using a AdoHcy standard curve.

## 5.9 | Cross-linking PRMT1 constructs

PRMT1 constructs (WT and TIM2) were desalted using Zeba Micro Spin Desalting columns (Thermo Fisher). Samples were prepared with 0.5 μM enzyme in 50 mM Na<sub>2</sub>HPO<sub>4</sub> (pH 7.6) along with H421 biotinylated peptide (0.25–0.5 μM). Samples were incubated at room temperature for 10 min before adding a final concentration of 0.025% glutaraldehyde (Sigma). Cross-linking controls were treated identically to samples, except water was added in place of glutaraldehyde. Cross-linking reactions were incubated for 10 min at 25°C before quenching with 1 M Tris-HCl (pH 7.5). 4× SDS-PAGE sample buffer was added to cross-linked samples before heating samples at 100°C for 5 min. Samples were run on a 4%–20% Mini-Protean TGX gel at 100 V. Gels were transferred to PVDF membrane and subjected to western blotting. The membrane was probed with 1:5000 precision protein StrepTactin-HRP (Bio-Rad) in 5% BSA in 1× TTBS.

## 5.10 | Binding affinity determination by isothermal spectral shift

Purified PRMT1 or TIM2 PRMT1 was labeled using Second Generation NHS-Red (NanoTemper) according to the manufacturer's suggested instructions. Sixteen two-fold serial dilutions of unlabeled PRMT1 starting from 3.25 μM were prepared in 50 mM Na<sub>2</sub>HPO<sub>4</sub> (pH 8.0), 1 mM DTT, and 1 mM EDTA. 20 nM of labeled PRMT was added to each of the dilutions, mixed thoroughly, and incubated for 15 min at room temperature to reach equilibrium. Samples were analyzed by Spectral Shift using a Monolith X device (NanoTemper). Data points ( $n = 4$ ) were fitted with MO. Control v2 software (NanoTemper) using the  $K_d$  model equation as follows:

$$f(c) = \text{Unbound} + (\text{Bound} - \text{Unbound}) \times \frac{c + c_{\text{target}} + K_d - \sqrt{(c + c_{\text{target}} + K_d)^2 - 4c c_{\text{target}}}}{2c_{\text{target}}}$$

where  $f(c)$  is the fraction bound at a given ligand concentration  $c$ ; Unbound is the signal of the target alone; Bound is the signal of the complex;  $K_d$  is the dissociation constant; and  $c_{\text{target}}$  is the final concentration of target in the assay.

## AUTHOR CONTRIBUTIONS

**Vincent Rossi:** Investigation; validation; visualization; writing—review and editing. **Sarah E. Nielson:** Investigation; validation; visualization; writing—review and editing. **Ariana Ortolano:** Investigation; visualization; validation; writing—review and editing. **Isabella Lonardo:** Investigation; validation; visualization; writing—review and editing. **Emeline Haroldsen:** Investigation; visualization; validation; writing—review and editing. **Drake Comer:** Investigation; validation; writing—review and editing. **Owen M. Price:** Visualization; writing—review and editing. **Nathan Wallace:** Investigation; writing—review and editing. **Joan M. Hevel:** Funding acquisition; conceptualization; writing—original draft; writing—review and editing; supervision; project administration.







## FUNDING INFORMATION

This work was supported by the National Science Foundation grants (CHE-2003769 to JH and MRI-1530862 to the Department of Chemistry & Biochemistry at USU) and by a Utah State University Undergraduate Research Creative Opportunities (URCO) Grant (to SN).

## CONFLICT OF INTEREST STATEMENT

The authors declare that they have no conflicts of interest with the contents of this article.

## ORCID

Vincent Rossi  <https://orcid.org/0009-0007-3157-9077>  
 Sarah E. Nielson  <https://orcid.org/0009-0009-8070-4350>  
 Isabella Lonardo  <https://orcid.org/0009-0002-6751-8018>  
 Emeline Haroldsen  <https://orcid.org/0009-0008-6785-4859>  
 Owen M Price  <https://orcid.org/0000-0001-5894-9022>  
 Joan M. Hevel  <https://orcid.org/0000-0002-9559-4635>

## REFERENCES

Adamopoulos PG, Mavrogiannis AV, Kontos CK, Scorilas A. Novel alternative splice variants of the human protein arginine

- methyltransferase 1 (PRMT1) gene, discovered using next-generation sequencing. *Gene*. 2019;699:135–44.
- Al-Hamashi AA, Diaz K, Huang R. Non-histone arginine methylation by protein arginine Methyltransferases. *Curr Protein Pept Sci*. 2020;21:699–712.
- Anon cancer.sanger.ac.uk/cosmic.
- Anon Human Protein Atlas. Available from: [proteintlas.org](http://proteintlas.org)
- Balint BL, Szanto A, Madi A, Bauer U-M, Gabor P, Benko S, et al. Arginine methylation provides epigenetic transcription memory for retinoid-induced differentiation in myeloid cells. *Mol Cell Biol*. 2005;25:5648–63.
- Boffa LC, Karn J, Vidali G, Allfrey VG. Distribution of NG, NG-dimethylarginine in nuclear protein fractions. *Biochem Biophys Res Commun*. 1977;74:969–76.
- Bujalowski W, Lohman TM. Monomer-tetramer equilibrium of the *Escherichia coli* ssb-1 mutant single strand binding protein. *J Biol Chem*. 1991;266:1616–26.
- Bulau P, Zakrzewicz D, Kitowska K, Leiper J, Gunther A, Grimminger F, et al. Analysis of methylarginine metabolism in the cardiovascular system identifies the lung as a major source of ADMA. *Am J Physiol Lung Cell Mol Physiol*. 2007;292:L18–24.
- Bulau P, Zakrzewicz D, Kitowska K, Wardega B, Kreuder J, Eickelberg O. Quantitative assessment of arginine methylation in free versus protein-incorporated amino acids in vitro and in vivo using protein hydrolysis and high-performance liquid chromatography. *Biotechniques*. 2006;40:305–10.
- Cao M-T, Feng Y, Zheng YG. Protein arginine methyltransferase 6 is a novel substrate of protein arginine methyltransferase 1. *World J Biol Chem*. 2023;14:84–98.
- Chen Y, Liang W, Du J, Ma J, Liang R, Tao M. PRMT6 functionally associates with PRMT5 to promote colorectal cancer progression through epigenetically repressing the expression of CDKN2B and CCNG1. *Exp Cell Res*. 2023;422:113413.
- Cheng Y, Frazier M, Lu F, Cao X, Redinbo MR. Crystal structure of the plant epigenetic protein arginine Methyltransferase 10. *J Mol Biol*. 2011;414:106–22.
- Dashti P, Lewallen EA, Gordon JAR, Montecino MA, van Leeuwen JPTM, Stein GS, et al. Protein arginine methyltransferases PRMT1, PRMT4/CARM1 and PRMT5 have distinct functions in control of osteoblast differentiation. *Bone Rep*. 2023;19:101704.
- Dong J, Duan J, Hui Z, Garrido C, Deng Z, Xie T, et al. An updated patent review of protein arginine N-methyltransferase inhibitors (2019-2022). *Expert Opin Ther Pat*. 2022;32:1185–205.
- Edwards GB, Muthurajan UM, Bowerman S, Luger K. Analytical ultracentrifugation (AUC): an overview of the application of fluorescence and absorbance AUC to the study of biological macromolecules. *Curr Protoc Mol Biol*. 2020;133:e131.
- Esse R, Imbard A, Florindo C, Gupta S, Quinlivan EP, Davids M, et al. Protein arginine hypomethylation in a mouse model of cystathionine  $\beta$ -synthase deficiency. *FASEB J*. 2014;28:2686–95.
- Feng G, Chen C, Luo Y. PRMT1 accelerates cell proliferation, migration, and tumor growth by upregulating ZEB1/H4R3-me2as in thyroid carcinoma. *Oncol Rep*. 2023;50:210.
- Feng Y, Xie N, Jin M, Stahley MR, Stivers JT, Zheng YG. A transient kinetic analysis of PRMT1 catalysis. *Biochemistry*. 2011;50:7033–44.
- Filipović J, Bosić M, Ćirović S, Životić M, Dunderović D, Đorđević D, et al. PRMT1 expression in renal cell tumors – application in differential diagnosis and prognostic relevance. *Diagn Pathol*. 2019;14:120.
- Frieden C. Protein oligomerization as a metabolic control mechanism: application to apoE. *Protein Sci*. 2019;28:837–42.
- Gao X, Pan W-S, Dai H, Zhang Y, Wu N-H, Shen Y-F. CARM1 activates myogenin gene via PCAF in the early differentiation of TPA-induced rhabdomyosarcoma-derived cells. *J Cell Biochem*. 2010;110:162–70.
- Goulet I, Gauvin G, Boisvenue S, Côté J. Alternative splicing yields protein arginine Methyltransferase 1 isoforms with distinct activity, substrate specificity, and subcellular localization. *J Biol Chem*. 2007;282:33009–21.
- Hartley A-V, Lu T. Modulating the modulators: regulation of protein arginine methyltransferases by post-translational modifications. *Drug Discov Today*. 2020;25:1735–43.
- He L, Hu Z, Sun Y, Zhang M, Zhu H, Jiang L, et al. PRMT1 is critical to FEN1 expression and drug resistance in lung cancer cells. *DNA Repair*. 2020;95:102953.
- Hein MY, Hubner NC, Poser I, Cox J, Nagaraj N, Toyoda Y, et al. A human Interactome in three quantitative dimensions organized by Stoichiometries and abundances. *Cell*. 2015;163:712–23.
- Herrmann F, Fackelmayer FO. Nucleo-cytoplasmic shuttling of protein arginine methyltransferase 1 (PRMT1) requires enzymatic activity. *Genes Cells*. 2009;14:309–17.
- Herrmann F, Pably P, Eckerich C, Bedford MT, Fackelmayer FO. Human protein arginine methyltransferases in vivo—distinct properties of eight canonical members of the PRMT family. *J Cell Sci*. 2009;122:667–77.
- Hevel JM, Price OM. Rapid and direct measurement of methyltransferase activity in about 30 min. *Methods*. 2020;175:3–9.
- Hobble HV, Schaner Tooley CE. Intrafamily heterooligomerization as an emerging mechanism of methyltransferase regulation. *Epigenetics Chromatin*. 2024;17:5.
- Hornbeck PV, Zhang B, Murray B, Kornhauser JM, Latham V, Skrzypek E. PhosphoSitePlus, 2014: mutations, PTMs and recalibrations. *Nucleic Acids Res*. 2015;43:D512–20.
- Hwang JW, Cho Y, Bae G-U, Kim S-N, Kim YK. Protein arginine methyltransferases: promising targets for cancer therapy. *Exp Mol Med*. 2021;53:788–808.
- Jarrold J, Davies CC. PRMTs and arginine methylation: Cancer's best-kept secret? *Trends Mol Med*. 2019;25:993–1009.
- Jia Y, Yu X, Liu R, Shi L, Jin H, Yang D, et al. PRMT1 methylation of WTAP promotes multiple myeloma tumorigenesis by activating oxidative phosphorylation via m6A modification of NDUFS6. *Cell Death Dis*. 2023;14:512.
- Jiang R, Shen H, Piao Y-J. The morphometrical analysis on the ultrastructure of A549 cells. *Romanian. J Morphol Embryol*. 2010;51:663–7.
- Kim M-S, Pinto SM, Getnet D, Nirujogi RS, Manda SS, Chaerkady R, et al. A draft map of the human proteome. *Nature*. 2014;509:575–81.
- Kooshapur H, Choudhury NR, Simon B, Mühlbauer M, Jussupow A, Fernandez N, et al. Structural basis for terminal loop recognition and stimulation of pri-miRNA-18a processing by hnRNP A1. *Nat Commun*. 2018;9:2479.
- Lambers C, Lei F, Tamm M, Hötzenecker K, Jaksch P, Roth M. Disease specific upregulation of protein arginine methyltransferases in IPF. *Eur Respir J*. 2019;54:PA2412. <https://doi.org/10.1183/13993003.congress-2019.PA2412>

- Lebowitz J, Lewis MS, Schuck P. Modern analytical ultracentrifugation in protein science: a tutorial review. *Protein Sci.* 2002;11:2067–79.
- Lee DY, Ianculescu I, Purcell D, Zhang X, Cheng X, Stallcup MR. Surface-scanning mutational analysis of protein arginine methyltransferase 1: roles of specific amino acids in methyltransferase substrate specificity, oligomerization, and coactivator function. *Mol Endocrinol.* 2007;21:1381–93.
- Lee J, Sayegh J, Daniel JA, Clarke SG, Bedford MT. PRMT8, a new membrane-bound tissue-specific member of the protein arginine methyltransferase family. *J Biol Chem.* 2005;280:32890–6.
- Lee W-C, Lin W-L, Matsui T, Chen ES-W, Wei T-YW, Lin W-H, et al. Protein arginine Methyltransferase 8: tetrameric structure and protein substrate specificity. *Biochemistry.* 2015;54:7514–23.
- Lei N, Zhang X, Chen H, Wang Y, Zhan Y, Zheng Z, et al. A feedback regulatory loop between methyltransferase PRMT1 and orphan receptor TR3. *Nucleic Acids Res.* 2009;37:832–48.
- Li X, Wang C, Jiang H, Luo C. A patent review of arginine methyltransferase inhibitors (2010-2018). *Expert Opin Ther Pat.* 2019;29:97–114.
- Liu J, Bu X, Chu C, Dai X, Asara JM, Sicinski P, et al. PRMT1 mediated methylation of cGAS suppresses anti-tumor immunity. *Nat Commun.* 2023;14:2806.
- Liu L, Lin B, Yin S, Ball LE, Delaney JR, Long DT, et al. Arginine methylation of BRD4 by PRMT2/4 governs transcription and DNA repair. *Sci Adv.* 2022;8:eadd8928.
- Liu L, Sun Q, Bao R, Roth M, Zhong B, Lan X, et al. Specific regulation of PRMT1 expression by PIAS1 and RKIP in BEAS-2B epithelia cells and HFL-1 fibroblasts in lung inflammation. *Sci Rep.* 2016;6:21810.
- Lorton BM, Shechter D. Cellular consequences of arginine methylation. *Cell Mol Life Sci.* 2019;76:2933–56.
- Maron MI, Lehman SM, Gayatri S, DeAngelo JD, Hegde S, Lorton BM, et al. Independent transcriptomic and proteomic regulation by type I and II protein arginine methyltransferases. *iScience.* 2021;24:102971.
- Mateus A, Matsson P, Artursson P. Rapid measurement of intracellular unbound drug concentrations. *Mol Pharm.* 2013;10:2467–78.
- Maxwell KL, Bona D, Liu C, Arrowsmith CH, Edwards AM. Refolding out of guanidine hydrochloride is an effective approach for high-throughput structural studies of small proteins. *Protein Sci.* 2003;12:2073–80.
- Messier V, Zenklusen D, Michnick SW. A nutrient-responsive pathway that determines M phase timing through control of B-cyclin mRNA stability. *Cell.* 2013;153:1080–93.
- Milo R. What is the total number of protein molecules per cell volume? A call to rethink some published values. *Bioessays.* 2013;35:1050–5.
- Morales Y, Cáceres T, May K, Hevel JM. Biochemistry and regulation of the protein arginine methyltransferases (PRMTs). *Arch Biochem Biophys.* 2016;590:138–52.
- Morales Y, Nitzel DV, Price OM, Gui S, Li J, Qu J, et al. Redox control of protein arginine Methyltransferase 1 (PRMT1) activity. *J Biol Chem.* 2015;290:14915–26.
- Moritz B, Lilie H, Naarmann-de Vries IS, Urlaub H, Wahle E, Ostareck-Lederer A, et al. Biophysical and biochemical analysis of hnRNP K: arginine methylation, reversible aggregation and combinatorial binding to nucleic acids. *Biol Chem.* 2014;395:837–53.
- Paik WK, Kim S. Protein methylation: chemical, Enzymological, and biological significance. *Advances in enzymology and related areas of molecular biology.* New Jersey: John Wiley & Sons, Ltd; 2006. p. 227–86. <https://doi.org/10.1002/9780470122877.ch5>
- Pak ML, Lakowski TM, Thomas D, Vhuyian MI, Hüsecken K, Frankel A. A protein arginine N-Methyltransferase 1 (PRMT1) and 2 Heteromeric interaction increases PRMT1 enzymatic activity. *Biochemistry.* 2011;50:8226–40.
- Pan W-A, Tsai H-Y, Wang S-C, Hsiao M, Wu P-Y, Tsai M-D. The RNA recognition motif of NIFK is required for rRNA maturation during cell cycle progression. *RNA Biol.* 2015;12:255–67.
- Park J-Y, Choi J-H, Lee S-N, Cho H-J, Ahn J-S, Kim Y-B, et al. Protein arginine methyltransferase 1 contributes to the development of allergic rhinitis by promoting the production of epithelial-derived cytokines. *J Allergy Clin Immunol.* 2021;147:1720–31.
- Patounas O, Papacharalampous I, Eckerich C, Markopoulos GS, Kolettas E, Fackelmayer FO. A novel splicing isoform of protein arginine methyltransferase 1 (PRMT1) that lacks the dimerization arm and correlates with cellular malignancy. *J Cell Biochem.* 2018;119:2110–23.
- Pawlak MR, Scherer CA, Chen J, Roshon MJ, Ruley HE. Arginine N-methyltransferase 1 is required for early postimplantation mouse development, but cells deficient in the enzyme are viable. *Mol Cell Biol.* 2000;20:4859–69.
- Price OM, Thakur A, Ortolano A, Towne A, Velez C, Acevedo O, et al. Naturally occurring cancer-associated mutations disrupt oligomerization and activity of protein arginine methyltransferase 1 (PRMT1). *J Biol Chem.* 2021;297:101336.
- Rowley MJ, Prout-Holm RA, Liu RW, Hendrickson-Rebizant T, Ige OO, Lakowski TM, et al. Protein arginine N-methyltransferase 2 plays a noncatalytic role in the histone methylation activity of PRMT1. *J Biol Chem.* 2023;299:105360.
- Rust HL, Zurita-Lopez CI, Clarke S, Thompson PR. Mechanistic studies on transcriptional coactivator protein arginine methyltransferase 1. *Biochemistry.* 2011;50:3332–45.
- Schapiro M, Ferreira de Freitas R. Structural biology and chemistry of protein arginine methyltransferases. *Medchemcomm.* 2014;5:1779–88.
- Schuck P. Size-distribution analysis of macromolecules by sedimentation velocity ultracentrifugation and lamm equation modeling. *Biophys J.* 2000;78:1606–19.
- Shen S, Zhou H, Xiao Z, Zhan S, Tuo Y, Chen D, et al. PRMT1 in human neoplasm: cancer biology and potential therapeutic target. *Cell Commun Signal.* 2024;22:102.
- Singh SS, Jois SD homo- and heterodimerization of proteins in cell signaling: inhibition and drug design. *Advances in protein chemistry and structural biology.* Volume 111. Pennsylvania: Elsevier; 2018. p. 1–59. Available from: <https://linkinghub.elsevier.com/retrieve/pii/S1876162317300640>
- Song C, Chen T, He L, Ma N, Li J, Rong Y-F, et al. PRMT1 promotes pancreatic cancer growth and predicts poor prognosis. *Cell Oncol.* 2020;43:51–62.
- Su H, Liu S-M, Sun C-W, Bedford MT, Zhao X. Protein arginine Methyltransferase 1 (PRMT1) dampens self-renewal and

- promotes differentiation of hematopoietic stem cells in mouse models. *Blood*. 2019;134:2460.
- Suh-Lailam BB, Hevel JM. A fast and efficient method for quantitative measurement of S-adenosyl-L-methionine-dependent methyltransferase activity with protein substrates. *Anal Biochem*. 2010;398:218–24.
- Sun Q, Liu L, Wang H, Mandal J, Khan P, Hostettler KE, et al. Constitutive high expression of protein arginine methyltransferase 1 in asthmatic airway smooth muscle cells is caused by reduced microRNA-19a expression and leads to enhanced remodeling. *J Allergy Clin Immunol*. 2017;140:510–524.e3.
- Takahama K, Kino K, Arai S, Kurokawa R, Oyoshi T. Identification of Ewing's sarcoma protein as a G-quadruplex DNA- and RNA-binding protein. *FEBS J*. 2011;278:988–98.
- Tang J, Frankel A, Cook RJ, Kim S, Paik WK, Williams KR, et al. PRMT1 is the predominant type I protein arginine Methyltransferase in mammalian cells. *J Biol Chem*. 2000;275:7723–30.
- Tate JG, Bamford S, Jubb HC, Sondka Z, Beare DM, Bindal N, et al. COSMIC: the catalogue of somatic mutations in cancer. *Nucleic Acids Res*. 2019;47:D941–7.
- Tewary SK, Zheng YG, Ho M-C. Protein arginine methyltransferases: insights into the enzyme structure and mechanism at the atomic level. *Cell Mol Life Sci CMLS*. 2019;76:2917–32.
- Thiebaut C, Eve L, Poulard C, Le Romancer M. Structure, activity, and function of PRMT1. *Life (Basel)*. 2021;11:1147.
- Thomas D, Lakowski TM, Pak ML, Kim JJ, Frankel A. Förster resonance energy transfer measurements of cofactor-dependent effects on protein arginine N-methyltransferase homodimerization. *Protein Sci*. 2010;19:2141–51.
- Toma-Fukai S, Kim J-D, Park K-E, Kuwabara N, Shimizu N, Krayukhina E, et al. Novel helical assembly in arginine methyltransferase 8. *J Mol Biol*. 2016;428:1197–208.
- Troffer-Charlier N, Cura V, Hassenboehler P, Moras D, Cavarelli J. Functional insights from structures of coactivator-associated arginine methyltransferase 1 domains. *EMBO J*. 2007;26:4391–401.
- Uhlén M, Fagerberg L, Hallström BM, Lindskog C, Oksvold P, Mardinoglu A, et al. Tissue-based map of the human proteome. *Science*. 2015;347:1260419.
- Wada K, Inoue K, Hagiwara M. Identification of methylated proteins by protein arginine N-methyltransferase 1, PRMT1, with a new expression cloning strategy. *Biochim. Biophys Acta BBA*. 2002;1591:1–10.
- Wang S-CM, Dowhan DH, Muscat GEO. Epigenetic arginine methylation in breast cancer: emerging therapeutic strategies. *J Mol Endocrinol*. 2019;62:R223–37.
- Weiss VH, McBride AE, Soriano MA, Filman DJ, Silver PA, Hogle JM. The structure and oligomerization of the yeast arginine methyltransferase, Hmt1. *Nat Struct Biol*. 2000;7:1165–71.
- Xu J, Richard S. Cellular pathways influenced by protein arginine methylation: implications for cancer. *Mol Cell*. 2021;81:4357–68.
- Yao B, Gui T, Zeng X, Deng Y, Wang Z, Wang Y, et al. PRMT1-mediated H4R3me2a recruits SMARCA4 to promote colorectal cancer progression by enhancing EGFR signaling. *Genome Med*. 2021;13:58.
- Yoshimatsu M, Toyokawa G, Hayami S, Unoki M, Tsunoda T, Field HI, et al. Dysregulation of PRMT1 and PRMT6, type I arginine methyltransferases, is involved in various types of human cancers. *Int J Cancer*. 2011;128:562–73.
- Zakrzewicz D, Zakrzewicz A, Didiysova M, Korenecak M, Kosanovic D, Schermuly RT, et al. Elevated protein arginine methyltransferase 1 expression regulates fibroblast motility in pulmonary fibrosis. *Biochim. Biophys Acta BBA*. 2015;1852:2678–88.
- Zakrzewicz D, Zakrzewicz A, Didiysova M, Preissner KT, Wygrecka M. Elevated protein arginine methyltransferase 1 expression contributes to the pathogenesis of pulmonary fibrosis. *Eur Respir J*. 2014;44:P3507. [https://erj.ersjournals.com/content/44/Suppl\\_58/P3507](https://erj.ersjournals.com/content/44/Suppl_58/P3507)
- Zhang F, Kerbl-Knapp J, Rodriguez Colman MJ, Meinitzer A, Macher T, Vujić N, et al. Global analysis of protein arginine methylation. *Cell Rep Methods*. 2021;1:100016.
- Zhang X, Cheng X. Structure of the predominant protein arginine methyltransferase PRMT1 and analysis of its binding to substrate peptides. *Structure*. 2003;11:509–20.
- Zhang X, Zhou L, Cheng X. Crystal structure of the conserved core of protein arginine methyltransferase PRMT3. *EMBO J*. 2000;19:3509–19.
- Zhou R, Xie Y, Hu H, Hu G, Patel VS, Zhang J, et al. Molecular mechanism underlying PRMT1 dimerization for SAM binding and Methylase activity. *J Chem Inf Model*. 2015;55:2623–32.
- Zhu Q, Wang D, Liang F, Tong X, Liang Z, Wang X, et al. Protein arginine methyltransferase PRMT1 promotes adipogenesis by modulating transcription factors C/EBP $\beta$  and PPAR $\gamma$ . *J Biol Chem*. 2022;298:102309.

## SUPPORTING INFORMATION

Additional supporting information can be found online in the Supporting Information section at the end of this article.

**How to cite this article:** Rossi V, Nielson SE, Ortolano A, Lonardo I, Haroldsen E, Comer D, et al. Oligomerization of protein arginine methyltransferase 1 and its effect on methyltransferase activity and substrate specificity. *Protein Science*. 2024;33(8):e5118. <https://doi.org/10.1002/pro.5118>